Biosensors and Bioelectronics 25 (2010) 2503–2508

Contents lists available at ScienceDirect

Biosensors and Bioelectronics

journal homepage: www.elsevier.com/locate/bios

Acetylcholinesterase biosensor design based on carbon nanotube-encapsulated polypyrrole and polyaniline copolymer for amperometric detection of organophosphates

Dan Du[a,*], Xiaoxue Ye[a], Jie Cai[b], Juan Liu[a], Aidong Zhang[a]

[a] Key Laboratory of Pesticide and Chemical Biology of Ministry of Education, College of Chemistry, Central China Normal University, Wuhan 430079, PR China
[b] The Technology Center of Wuhan Iron & Steel Company, Wuhan 430080, PR China

ARTICLE INFO

Article history:
Received 2 February 2010
Received in revised form 14 April 2010
Accepted 14 April 2010
Available online 22 April 2010

Keywords:
Polypyrrole-polyaniline copolymer
Carbon nanotubes
Organophosphates
Acetylcholinesterase
Biosensor

ABSTRACT

A simple method to immobilize acetylcholinesterase (AChE) on polypyrrole (PPy) and polyaniline (PANI) copolymer doped with multi-walled carbon nanotubes (MWCNTs) was proposed. The synthesized PAn-PPy-MWCNTs copolymer presented a porous and homogeneous morphology which provided an ideal size to entrap enzyme molecules. Due to the biocompatible microenvironment provided by the copolymer network, the obtained composite was devised for AChE attachment, resulting in a stable AChE biosensor for screening of organophosphates (OPs) exposure. MWCNTs promoted electron-transfer reactions at a lower potential and catalyzed the electro-oxidation of thiocholine, thus increasing detection sensitivity. Based on the inhibition of OPs on the AChE activity, using malathion as a model compound, the inhibition of malathion was proportional to its concentration ranging from 0.01 to 0.5 μg/mL and from 1 to 25 μg/mL, with a detection limit of 1.0 ng/mL. The developed biosensor exhibited good reproducibility and acceptable stability, thus providing a new promising tool for analysis of enzyme inhibitors.

1. Introduction

Organophosphates (OPs) have been widely used as pesticides in modern agriculture due to their low persistence and high insecticidal activity (Young et al., 2004; Wang and Lin, 2008). However, long-term accumulations in environment, OPs contaminations have raised serious public concern regarding the food safety and human health (Wang et al., 2009; Scott et al., 1999). Numerous analysis methods including gas chromatography (Frenich et al., 2005), liquid chromatography (Cappielo et al., 2002), ultraviolet spectroscopy (Ganzera et al., 2006), gas-mass spectroscopy (Wong et al., 2007), fluorimetry (Dams et al., 2002) and surface plasmon resonance (SPR) (Chand and Gupta, 2007) have been developed to assess OPs exposures. Although these methods could quantitatively provide an accurate evaluation of the health risk of integrated OPs exposure, they still suffer from some intrinsic disadvantages of either low detection specificity and sensitivity, or expensive analysis settings entailing well-trained personnel and inconvenience for field applications. Hence, simple, sensitive, selective, and field-deployable tools are still highly desired for biomonitoring and diagnostic evaluation of OP exposures.

Amperometric acetylcholinesterase (AChE) biosensors present a promising alternative to the traditional methods due to their good selectivity, sensitivity, rapid response, and miniature size. AChE biosensors have shown satisfactory results for pesticides analysis (Du et al., 2007a, 2010), in which the enzymatic activity is employed as an indicator of quantitative measurement of insecticides. In this regard, immobilization of enzyme to an electrode surface without its bioactivity being sacrificed is a crucial step for the design of the biosensors (Gill and Ballesteros, 2000). Usual methods of immobilization include direct physical adsorption onto a solid support (Sotiropoulou and Chaniotakis, 2005), encapsulation into a hydrogel (Yadavalli et al., 2004), cross-linking (Solna et al., 2005), and covalent binding (Lin et al., 2004). The conducting polymers have attracted much attention due to their interesting electrical and electrochemical properties (Mu et al., 1997). Among them, polyaniline (PAn) and polypyrrole (PPy) gain their popularities by exhibiting relatively high conductivity, easy preparation, and excellent environmental stability (Hong and Park, 2005; Zhong et al., 2006). Their most promising applications are electrochemical biosensing, as they can provide suitable environment for immobilization of biomolecules and act as mediator (Luo et al., 2006; Kim et al., 2000). Recently, copolymers composites were also prepared successfully (Kojima et al., 1995; Cho et al., 2004). The syntheses can be achieved either by electrolyzing the solution including two monomers or by two-step electropolymerization (Cakmak et al., 2005). In the second method, the first monomer is

* Corresponding author. Tel.: +86 27 67867958.
E-mail address: dudan@mail.ccnu.edu.cn (D. Du).

0956-5663/$ – see front matter © 2010 Elsevier B.V. All rights reserved.
doi:10.1016/j.bios.2010.04.018

electrochemically polymerized on the electrode surface and it is used as an electrode for the polymerization of second monomer. The main motivation for preparing copolymer composites lies in the possibility that the resulting product will not only display better properties than that of homopolymers and also overcome the limitation of the rareness of new conjugated π-bond-containing monomers (Choi and Park, 2000). In the recent years, copolymers incorporated with nanomaterials such as carbon nanotubes (CNTs) have been largely prepared. The resulting nanocomposites not only embodied the merits of the different components, which can widen the application fields than the neat ones but also exhibited enhancement of electrical ability as well as mechanical properties compared with pure conducting polymer or nanomaterials (Star et al., 2001; Chen et al., 1998; Arduini et al., 2006; Li et al., 2007).

In this paper, electrochemically formed copolymers were synthesized by subsequent electropolymerization of PPy and PAn on CNTs modified electrode for immobilization of AChE, leading to a stable AChE sensor for rapid determination of malathion, a model compound of OPs pesticides, quantitatively. The surface hydrophilicity was improved greatly after forming a complex structure instead of a separate layer. It provided an excellent environmental and chemical stability around the enzyme molecule to stabilize its biological activity to a large extent. The presence of nanoparticles not only promoted electron-transfer reactions and catalyzed the electro-oxidation of thiocholine, but also increased the surface area to capture a large amount of enzymes, thus increasing detection sensitivity.

2. Experimental

2.1. Reagents

AChE (Type C3389, 500 U/mg from electric eel), Acetylthiocholine chloride (ATCl) and pralidoxime iodide were purchased from Sigma–Aldrich (St. Louis, USA) and used as received. Malathion was obtained from AccuStandard (USA). Multi-walled carbon nanotubes (MWCNTs, Shenzhen Nanotech Port Co. Ltd., China) were used with further purification. Pyrrole and aniline were obtained from Aldrich and purified twice by distillation under the protection of high purity nitrogen and then kept in refrigerator before use. Other reagents, including sodium dodecyl sulfate (SDS) and phosphate buffer saline (PBS, pH 7.0) were of analytical reagent grade.

2.2. Instruments

Electrochemical measurements were performed on CHI-660C workstation (Shanghai Chenhua Instrument Corporation, China) with a conventional three-electrode system comprising platinum wire as auxiliary electrode, saturated calomel electrode (SCE) as reference and PAn-PPy-MWCNTs composite attaching AChE modified glassy carbon electrode (AChE/PAn-PPy-MWCNTs/GCE) as working electrode. Electrochemical impedance measurements were carried out in 5 mM $Fe(CN)_6^{4-/3-}$ with frequencies from 0.01 Hz to 100 kHz at open-circuit potential with an amplitude of 5 mV. Attenuated total reflection Fourier-transform infrared spectra (ATR-FTIR) were recorded on a Nexus 470 FTIR (Nicolet, USA) equipped with an omni sampler over 32 scans. Scanning electron microscopy (SEM) images were performed on a LEO 1450VP (Japan) scanning electron microscope.

2.3. Preparation of AChE/PAn-PPy-MWCNTs/GCE

A GCE was carefully polished carefully to a mirrorlike with 0.3- and 0.05-μm Al_2O_3 paste and washed sonication with ethanol and water. Before modification, a potential of +1.75 V was applied to the electrode, with stirring in pH 5.0 acetate buffer for 300 s and then scanned from +0.3 to +1.25 V and from +0.3 to −1.3 V until a steady curve was obtained. After this treatment, a large amount of oxygen-containing functional groups were formed on the surface of glass carbon electrode during the electrochemical activation. Some change in color was observed and a hydrophilic surface of the electrode was obtained (Du et al., 2007c).

The MWCNTs were refluxed in HNO_3 for 10 h. The resulting suspension was diluted with 500 mL water and centrifuged. The functional MWCNTs were washed for several times and dried at 60 °C overnight. For electrochemical deposition, the functional MWCNTs were added into 0.1 M SDS solution for ultrasonication about 1 h to form a uniform solution (Islam et al., 2003). Then, 0.1 M pyrrole was dissolved in this emulsion solution under ultrasonic stirring for 15 min at room temperature and electrochemically deposited on the GCE by CV from −0.2 to 0.8 V for eight circles. The obtained modified electrode, denoted as PPy-MWCNTs/GCE, was gently washed with distilled water to remove any non-adsorbed species. The PAn film was subsequently grown on the PPy-MWCNTs/GCE surface from 0.5 M aniline in 1.0 M H_2SO_4 by electropolymerization in the potential range from −0.2 to 0.8 V for eight cycles. The resulting PAn-PPy-MWCNTs nanocomposite modified electrode was rinsed carefully with water and dried at room temperature for 1 h. After evaporation of water, it was coated with 3.0 μL AChE and incubated at 25 °C for 30 min to obtain the AChE/PAn-PPy-MWCNTs/GCE. The biosensor was stored at 4 °C when not in use.

2.4. Measurement procedure

For detection of malathion, the obtained AChE/PAn-PPy-MWCNTs/GCE was first immersed in PBS containing different concentrations of standard malathion for 15 min, and then transferred to the electrochemical cell of 1.0 mL pH 7.0 PBS containing 0.3 mM ATCl to study the electrochemical response by cyclic voltammetry (CV). The inhibition of malathion was calculated as follows:

$$I\% = \frac{i_{P,control} - i_{P,exp}}{i_{P,control}} \times 100\%$$

where $i_{P,control}$ and $i_{P,exp}$ were peak currents of ATCl on AChE/PAn-PPy-MWCNTs/GCE before and after exposure to malathion, respectively.

Enzyme reactivation: after the AChE/PAn-PPy-MWCNTs/GCE was inhibited by malathion, it was washed with PBS and reactivated with 4.0 mM pralidoxime iodide for 8 min, then transferred to electrochemical cell of 1.0 mL pH 7.0 PBS containing 0.3 mM ATCl to study the electrochemical response. The reactivation efficiency (*R*%) was estimated as follows:

$$R\% = \left(\frac{i_r - i_{P,exp}}{i_{P,control} - i_{P,exp}} \right) \times 100\%$$

where i_r was the peak current of ATCl on AChE/PAn-PPy-MWCNTs/GCE after pralidoxime iodide reactivation.

3. Results and discussion

3.1. FTIR analysis

Fig. 1 showed the FTIR spectra of pure PAn (a), PPy-MWCNTs (b) and PAn-PPy-MWCNTs copolymer (c). In the spectrum of PAn, the characteristic peaks at 1570, 1540 and 1496 cm^{-1} (curve a) are attributed to the C=C stretching of quinoid and benzene ring, respectively (Su et al., 2007). Those at 1142 and 1082 cm^{-1} belong to C—N stretching of the secondary aromatic amine. From the spec-

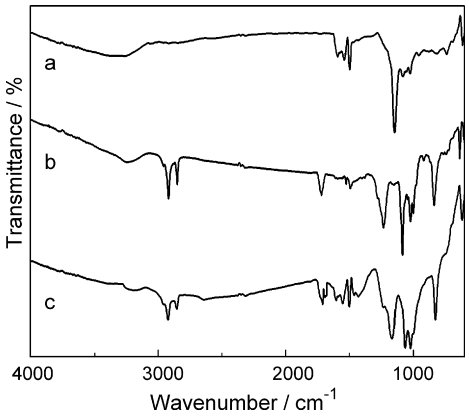

Fig. 1. FTIR spectra of pure PAn (a), PPy-MWCNTs (b) and PAn-PPy-MWCNTs copolymer (c).

trum of PPy-MWCNTs presented in curve b, the peaks at 1557 and 1232 cm^{-1} are due to C=C and C—N stretching, respectively (Mohammadi et al., 1986; Watanabe et al., 1981). The peaks at 1713 cm^{-1} is associated with the C=O stretching of the –COOH group present in MWCNTs (Kuznetsova et al., 2000). Other prominent feature for PPy-MWCNTs film was observed between 2840 and 2925 cm^{-1}, which can be assigned to the alkyl from SDS. The FIIR spectrum of PAn-PPy-MWCNTs copolymer (curve c) presents all the prominent features of PAn and PPy, which reveals the existence of both PAn and PPy in the copolymer film.

3.2. SEM characterization

The morphology of PPy-MWCNTs (A), PAn-MWCNTs (B) and PAn-PPy-MWCNTs nanocomposite (C) were characterized by SEM, as shown in Fig. 2. It can be clearly seen that the PPy-MWCNTs film present a rather porous and homogeneous morphology, which may be attributed to the incorporation of MWCNTs and SDS into the PPy film during electropolymerization. According to previous studies (Kamat et al., 2004; Kumar et al., 2004), pyrrole monomers could enter the interiors of SDS-encapsulated MWCNTs and locate at the interfaces between surfactants and CNTs. If a positive voltage was added to GCE, these SDS-encapsulated MWCNTs nanostructures would orient towards the surface of electrode. PPy located at the interfaces between SDS and MWCNTs could be electropolymerized at GCE and CNTs to form a porous and homogeneous PPy-MWCNTs film (Zhang et al., 2004a,b,c). It was also found that CV scans less than eight circles resulted in thin and unstable film. However, longer scans more than eight circles resulted in tight attachment of thick pyrrole films, which blocked the electron transfer of the substrate. Thus, electrochemical deposition of pyrrole on the electrode by CV scans for eight circles was selected for preparation of PPy-MWCNTs/GCE interface. If aniline monomers were directly electropolymerized with SDS-encapsulated MWCNTs, the resulting PAn-MWCNTs displayed a totally different morphology in which some uniform spots like structure was observed (B). However, subsequent electropolymerization of aniline on PPy-MWCNTs film resulted in a uniform morphology, indicating a well-packed, homogeneous PAn-PPy-MWCNTs nanocomposite was formed on the electrode surface, as shown in Fig. 2C. This produced nanostructure provides an ideal size to entrap enzyme molecules.

3.3. Electrochemical impedance measurements

Electrochemical impedance spectroscopy (EIS) is a powerful tool for mechanistic analysis of interfacial processes and for evaluating impedance changes. In EIS, the semicircle diameter equals the electron-transfer resistance, R_{ct}. This resistance controls the

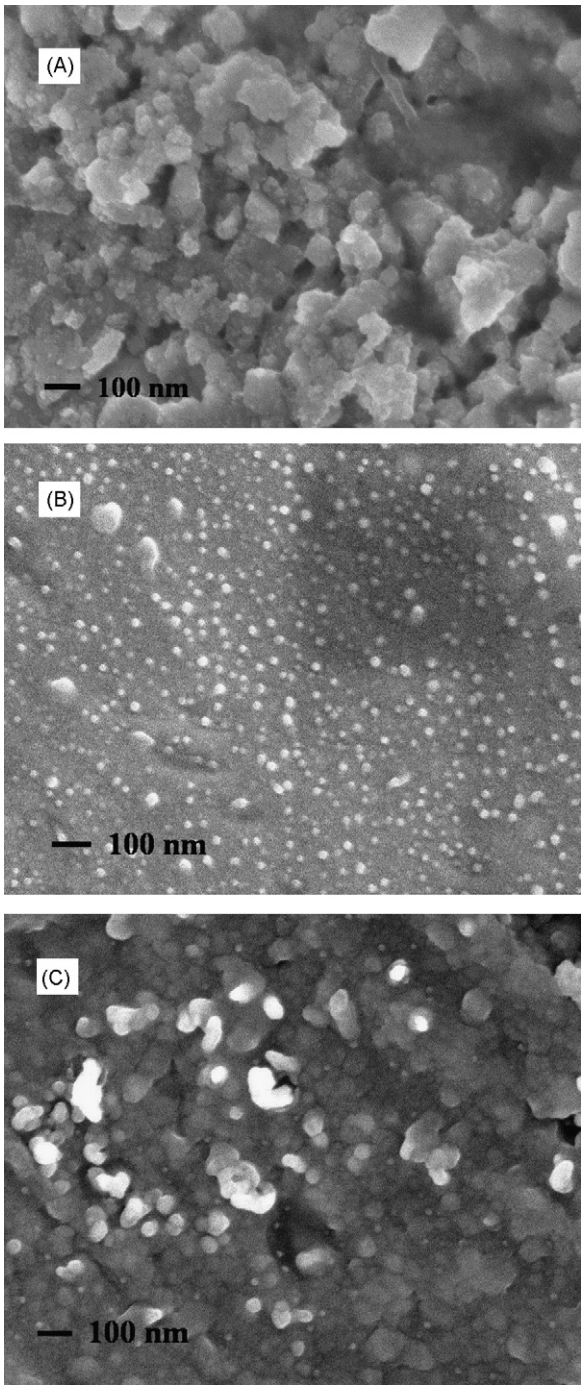

Fig. 2. SEM images of PPy-MWCNTs (A), PAn-MWCNTs (B) and PAn-PPy-MWCNTs composite (C).

electron-transfer kinetics of the redox probe at the electrode interface. Fig. 3A illustrated typical Nyquist plots obtained from bare GCE (a), PAn-PPy-MWCNTs/GCE (b) and AChE-PAn-PPy-MWCNTs/GCE (c) at the open-circuit potential using $Fe(CN)_6^{3-/4-}$ as the redox probe. A very small interfacial resistance on bare GCE was exhibited. When PAn-PPy-MWCNTs nanocomposites were formed on the electrode, we were surprised to observe an almost straight line (curve b). The R_{ct} was largely decreased even lower than that of a bare GCE. It is the characteristic of a mass diffusion limiting electron-transfer process. This result indicates that the electron transfer on the PAn-PPy-MWCNTs/GCE was very fast. The use of MWCNTs makes the electrochemical detection of the products from enzymatic reactions more feasible and promotes electron transfer

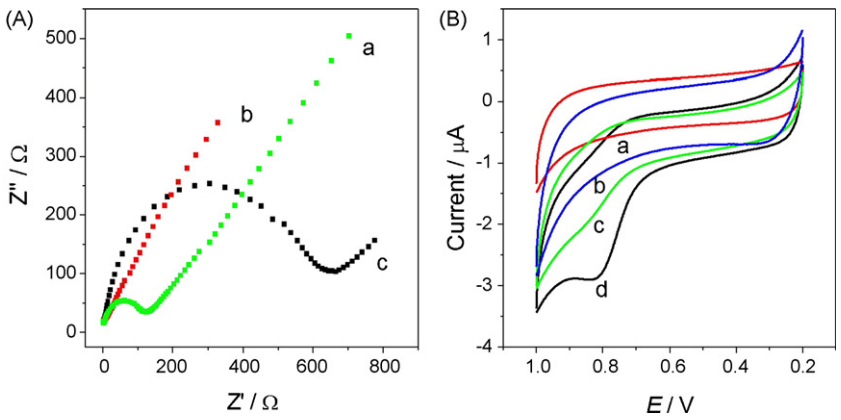

Fig. 3. (A) Electrochemical impedance spectra of bare GCE (a), PAn-PPy-MWCNTs/GCE (b) and AChE-PAn-PPy-MWCNTs/GCE (c) in 5 mM $K_3Fe(CN)_6$ and $K_4Fe(CN)_6$. (B) Cyclic voltammograms of bare GCE (a) and AChE-PAn-PPy-MWCNTs/GCE (b) in pH 7.0 PBS; AChE-PAn-PPy/GCE without MWCNTs (c) and AChE-PAn-PPy-MWCNTs/GCE (d) in pH 7.0 PBS containing 0.3 mM ATCl. Scan rate: 50 mV/s.

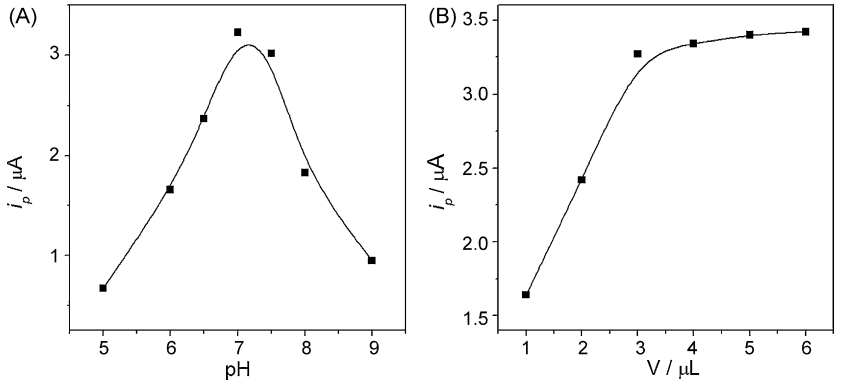

Fig. 4. Effect of the pH (A) and the volume of immobilized AChE (B) on the amperometric response.

due to their excellent and unique electronic properties. However, after the immobilization of AChE on the electrode surface, the interfacial resistance increased to 637 Ω (curve c) due to the increase of the thickness of the interface. The phenomenon was consistent with the fact that the protein layer insulated the conductive support and blocked the interfacial electron transfer. This was the direct evidence of successful binding of enzyme on the electrode surface.

3.4. Electrochemical behavior of AChE-PAn-PPy-MWCNTs/GCE

As shown in Fig. 3B, no peak was observed at bare GCE (curve a) and AChE-PAn-PPy-MWCNTs/GCE (curve b) in pH 7.0 PBS. When 0.3 mM ATCl was added to the PBS, the cyclic voltammogram of AChE-PAn-PPy-MWCNTs/GCE showed an irreversible oxidation peak at 797 mV (curve d) whereas no detectable signal was observed for PAn-PPy-MWCNTs/GCE (data not shown). Obviously this peak arose from the oxidation of thiocholine, which is the hydrolysis product of ATCl catalyzed by the immobilized AChE. This peak was much higher than that on the AChE-PAn-PPy/GCE without MWCNTs (curve c). This was due to the presence of MWCNTs in nanocomposite film, which possessed inherent conductive properties and catalytic behavior, thus it can provide a conductive pathway to electron transfer. The improvement in the response of the electrode could also be attributed to the increased the surface area in the presence of MWCNTs to capture a large amount of enzymes, thus amplifying the current response. The peak current of thiocholine on the AChE-PAn-PPy-MWCNTs/GCE increased with increasing the scan rate and the peak potential shifted slightly. The peak currents exhibited a linear dependence on the scan rate ranging from 10 to 200 mV/s (data not shown), indicating a typical surface-controlled electrode process. The formed PAn-PPy-MWCNTs nanocomposite provided an excellent environmental and chemical stability around the enzyme molecule to stabilize its biological activity to a large extent. The enzyme molecules were immobilized successfully on the electrode surface without leakage. Furthermore, the peak current observed in the simple electronic voltammetric sensing system reflected the activity of immobilized enzyme, which could be used as an indicator for quantitative measurement of OPs involved in the inhibition action.

3.5. Optimization parameters of the biosensor performance

The peak current was greatly influenced by the pH of the detection solution from 5.0 to 9.0 and the maximum response was observed at pH 7.0 (Fig. 4A). It was close to that previous report for

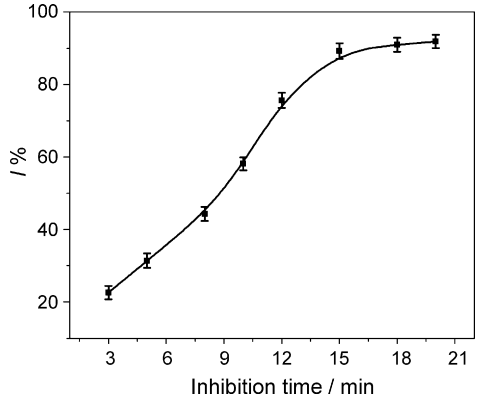

Fig. 5. Effect of inhibition time on inhibition efficiency.

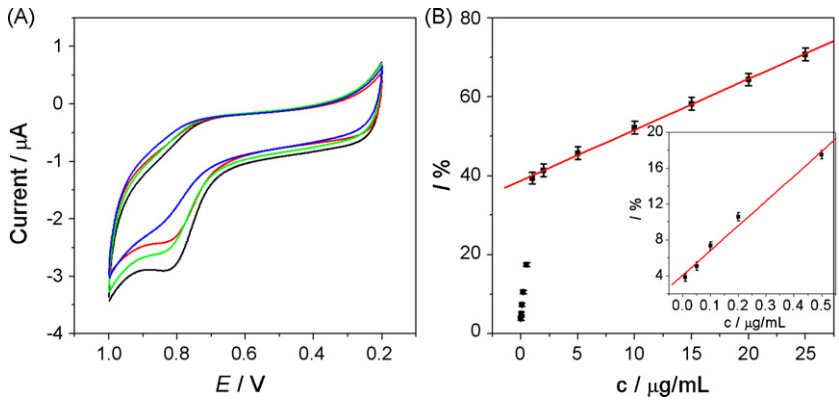

Fig. 6. (A) Cyclic voltammograms of AChE-PAn-PPy-MWCNTs/GCE in pH 7.0 PBS containing 0.3 mM ATCl (a) and after inhibition by malathion of different concentrations of 0.5 μg/mL (b), 2.0 μg/mL (c) and 20 μg/mL (d). (B) Relationship between inhibitions and concentrations of malathion. Inset: linear relationship between low inhibitions and low concentrations.

free AChE, indicating that copolymer film did not alter the optimal pH for catalytic behavior of AChE and the microenvironment surrounding immobilized enzyme was easily accessed by substrate (Bernabei et al., 1993). Thus, pH 7.0 was used in the detection solution.

The loading amount of AChE on electrode surface was another important parameter affects the amperometric response. With increasing the volume of AChE on the electrode, the signal from substrate increased quickly and maintained this value at the volume of 3.0 μL (Fig. 4B). It can be explained that as a result of imitation of electrode area, more than 3.0 μL enzyme adsorbing were not enough stable, indicating a saturation of enzyme loading. Therefore, a volume of 3.0 μL of AChE is chosen as the optimal volume for preparation of the biosensor.

3.6. Effect of malathion on response of AChE/PAn-PPy-MWCNTs/GCE

Upon the constructed AChE-PAn-PPy-MWCNTs/GCE was immersed in the standard solution of malathion at a known concentration, the produced current decreased drastically. Malathion displayed increasing inhibition on AChE with increasing the inhibition time (Fig. 5). The inhibition curve trended to a stable value when the incubation time was longer than 15 min. However, the maximum value of inhibition of malathion was not 100%, which indicated that the binding sites between pesticides and enzymes could reach saturation and equilibrium.

3.7. Calibration curve

Upon construction AChE-PAn-PPy-MWCNTs/GCE was immersed in the standard solution of malathion at a known concentration for 15 min, the produced current decreased drastically (Fig. 6A). This was because malathion as one of the OPs pesticides exhibited fairly high acute toxicity and involved in the irreversible inhibition action on AChE, thus reduced the enzymatic activity to its substrate. Due to the notable change in voltammetric signal of the AChE-PAn-PPy-MWCNTs/GCE, a simple method for determination of malathion was established. With an increase concentration of malathion concentration, the peak current decreased. Under the optimal experimental conditions, the inhibitions of malathion on AChE-PAn-PPy-MWCNTs/GCE were proportional to its concentrations in two ranges, from 0.01 to 0.5 μg/mL and from 1 to 25 μg/mL. The regression equation was $I\% = 27.65c + 4.07$ and $I\% = 1.28c + 38.84$, with the correlation coefficients of 0.9927 and 0.9994, respectively (Fig. 6B). The detection limit was 1.0 ng/mL, which is comparable to our previous studies (Du et al., 2007b). Furthermore, the inhibition rate of malathion decreased when increasing the concentration of malathion, indicating that the binding sites between pesticides and enzymes could reach saturation and equilibrium.

3.8. Reactivation

A crucial problem for practical applications is the strong inhibition on AChE, which limits the reuse of biosensor. In order to settle this problem, reactivation of the enzyme by oximes has been investigated (Du et al., 2009; Chen et al., 2005). The AChE/PAn-PPy-MWCNTs/GCE inhibited by OPs can be completely reactivated when using nucleophilic compounds such as pralidoxime iodide. With increasing reactivation time, the reactivation efficiency increased and reached a constant value after 8 min. The inhibited AChE could be regenerated more than 90% of its original activity after immerging in 4.0 mM pralidoxime iodide. Based on this reactivation procedure, the proposed biosensor can be used repeatedly with an acceptable reproducibility.

3.9. Precision of measurements and stability of biosensor

The inter-assay precision was estimated through determining the response of 0.3 mM ATCl at five different electrodes, which were immersed in 0.1 and 5.0 μg/mL malathion for 15 min, respectively. Similarly, the intra-assay precision of the biosensors was evaluated by assaying one enzyme electrode for five replicate determinations. The RSD of inter-assay and intra-assay were found to be 2.3% and 7.8%, respectively, indicating acceptable precision and reproducibility. When the enzyme electrode was not in use, it was stored in a refrigerator at 4 °C in dry condition for 2 weeks, no obvious decrease in the response of ATCl was observed. After a 30-day storage period, the sensor retained 85% of its initial current response. It indicated that copolymer interface provided a biocompatible microenvironment around the enzyme to stabilize its biological activity to a large extent.

4. Conclusions

In this work, well-packed, homogeneous PAn-PPy-MWCNTs copolymers were synthesized by subsequent electropolymerization strategy for immobilization of AChE, leading to a stable AChE biosensor for rapid determination of OPs quantitatively. The constructed copolymer network incorporating MWCNTs provided a biocompatible microenvironment around the enzyme molecules to stabilize their biological activity and prevented them from leaking out of the interface. Due to the fast electron transfer of MWCNTs,

the resulting AChE biosensor exhibited high affinity to its substrate and produced a detectable and fast response. Based on the notable change in voltammetric signal, the simple method for screening of OPs exposure was established. The resulting AChE biosensor exhibited high sensitivity, good reproducibility, long-term stability and low-cost processes, which provided a new promising tool for the characterization of enzyme inhibitors and pesticide analysis. This method for preparation of biosensor was "green", "low-cost", and more importantly, did not involve the use of any cytotoxic agent. The most difficult problem should focus on improving selectivity of AChE biosensor for pesticide detection. We are also currently facing the challenges of semi-automated procedures, which could be achieved through further improvement in miniaturization of electrochemical system.

Acknowledgements

The authors are gratefully acknowledging the financial support of the National Natural Science Foundation of China (no. 20705010) and the Research Fund for the Doctoral Program of Higher Education of China (no. 20070511015).

References

Arduini, F., Ricci, F., Tuta, C.S., Moscone, D., Amine, A., Palleschi, G., 2006. Anal. Chim. Acta 580, 155–162.
Bernabei, M., Chiavarii, S., Cremisini, C., Palleschi, G., 1993. Biosens. Bioelectron. 8, 265–271.
Cakmak, G., Kucukyavuz, Z., Kucukyavuz, S., 2005. Synth. Met. 151, 10–18.
Cappielo, A., Famiglini, G., Palma, P., Mangani, F., 2002. Anal. Chem. 74, 3547–3554.
Chand, R.S., Gupta, B.D., 2007. Sens. Actuat. B 123, 661–666.
Chen, J., Du, D., Yan, F., Ju, H.X., Lian, H.Z., 2005. Chem. Eur. J. 11, 1467–1472.
Chen, J., Hamon, M.A., Hu, H., Chen, Y., Rao, A.M., Eklund, P.C., Hadden, R.C., 1998. Science 282, 95–98.
Cho, C.H., Choi, H.J., Kim, J.W., Jhon, M.S., 2004. J. Mater. Sci. 39, 1883–1885.
Choi, S.J., Park, S.M., 2000. Adv. Mater. 12, 1547–1549.
Dams, R., Benijts, T., Lambert, W.E., De Leenheer, A.P., 2002. J. Chromatogr. B 773, 53–61.
Du, D., Chen, S.Z., Cai, J., Zhang, A.D., 2007a. Biosens. Bioelectron. 23, 130–134.
Du, D., Chen, W.J., Zhang, W.Y., Liu, D.L., Li, H.B., Lin, Y.H., 2010. Biosens. Bioelectron. 25, 1370–1375.
Du, D., Ding, J.W., Cai, J., Zhang, A.D., 2007b. J. Electroanal. Chem. 605, 53–60.
Du, D., Huang, X., Cai, J., Zhang, A.D., Ding, J.W., Chen, S.Z., 2007c. Anal. Bioanal. Chem. 387, 1059–1065.
Du, D., Wang, J., Smith, J.N., Timchalk, C., Lin, Y.H., 2009. Anal. Chem. 81, 9314–9320.
Frenich, A.G., Gonzalez-Rodrıguez, M.J., Arrebola, F.J., Martınez Vidal, J.L., 2005. Anal. Chem. 77, 4640–4648.
Ganzera, M., Aberham, A., Stuppner, H., 2006. J. Agric. Food Chem. 54, 3768–3772.
Gill, I., Ballesteros, A., 2000. Trends Biotechnol. 18, 282–296.
Hong, S.Y., Park, S.M., 2005. J. Phys. Chem. B 109, 9305–9310.
Islam, M.F., Rojas, E., Bergey, D.M., Johnson, A.T., Yodh, A.G., 2003. Nano Lett. 3, 269–273.
Kamat, P.V., Thomas, K.G., Barazzouk, S., Girishkumar, G., Vinodgopal, K., Meisel, D., 2004. J. Am. Chem. Soc. 126, 10757–10762.
Kim, J.H., Cho, J.H., Cha, G.S., 2000. Biosens. Bioelectron. 14, 907–915.
Kojima, T., Hayakawa, H., Tsuchiya, M., Kai, Y., 1995. J. Appl. Polym. Sci. 55, 1855–1859.
Kumar, M.S., Kim, T.H., Lee, S.H., Song, S.M., Yang, J.W., Nahm, K.S., Suh, E.K., 2004. Chem. Phys. Lett. 383, 235–239.
Kuznetsova, A., Mawhinney, D.B., Naumenko, V., Yates Jr., J.T., Liu, J., Smalley, R.E., 2000. Chem. Phys. Lett. 321, 292–296.
Li, B.X., He, Y.Z., Xu, C.L., 2007. Talanta 72, 223–230.
Lin, Y., Lu, F., Wang, J., 2004. J. Electroanal. Chem. 16, 145–149.
Luo, X.L., Killard, A.J., Morrin, A., Smyth, M.R., 2006. Anal. Chim. Acta 575, 39–44.
Mohammadi, A., Hasan, M.A., Liedberg, B., Lundstrom, I., Salaneck, W.R., 1986. Synth. Met. 14, 189–197.
Mu, S., Chen, C., Wang, J., 1997. Synth. Met. 88, 249–254.
Scott, G., Fulton, M., Moore, D., Wirth, E., Chandler, G., Key, P., Daugomah, J., Strozier, E., Devane, J., Clark, J., Lewis, M., Finley, D., Ellenberg, W., Karnaky, K., 1999. Toxicol. Ind. Health 15, 200–213.
Solna, R., Dock, E., Christenson, A., Winther-Nielsen, M., Carlsson, C., Emneus, J., Ruzgas, T., Skladal, P., 2005. Anal. Chim. Acta 528, 9–19.
Sotiropoulou, S., Chaniotakis, N.A., 2005. Anal. Chim. Acta 530, 199–204.
Star, A., Stoddart, J.F., Steuerman, D., Diehl, M., Boukai, A., Wong, E.W., Yang, X., Chung, S.W., Choi, H., Heath, J.R., 2001. Angew. Chem. Int. Ed. 40, 1721–1725.
Su, C., Wang, G., Huang, F., 2007. J. Appl. Polym. Sci. 106, 4241–4247.
Wang, J., Lin, Y.H., 2008. TrAC-Trend. Anal. Chem. 27, 619–626.
Wang, H., Wang, J., Choi, D., Tang, Z.W., Wu, H., Lin, Y.H., 2009. Biosens. Bioelectron. 24, 2377–2383.
Watanabe, A., Tanaka, M., Tanaka, J., 1981. Bull. Chem. Soc. Jpn. 54, 2278–2281.
Wong, J.W., Hennessy, M.K., Hayward, D.G., Krynitsky, A.J., Cassias, I., Schenck, F.J., 2007. J. Agric. Food Chem. 55, 1117–1128.
Yadavalli, V.K., Koh, W.G., Lazur, G.J., Pishko, M.V., 2004. Sens. Actuat. B 97, 290–297.
Young, S., Balluz, L., Malilay, J., 2004. Sci. Total Environ. 322, 320.
Zhang, M., Yan, Y., Gong, K., Mao, L., Guo, Z., Chen, Y., 2004a. Langmuir 20, 8781–8785.
Zhang, X., Zhang, J., Wang, R., Liu, Z., 2004b. Carbon 42, 1455–1461.
Zhang, X., Zhang, J., Wang, R., Zhu, T., Liu, Z., 2004c. Chem. Phys. Chem. 5, 998–1002.
Zhong, W., Liu, S., Chen, X., Wang, Y., Yang, W., 2006. Macromolecules 39, 3224–3230.